Focal adhesions are sites of integrin extension

Janet A. Askari,[1] Christopher J. Tynan,[2] Stephen E.D. Webb,[2] Marisa L. Martin-Fernandez,[2] Christoph Ballestrem,[1] and Martin J. Humphries[1]

[1]Wellcome Trust Centre for Cell-Matrix Research, Faculty of Life Sciences, University of Manchester, Manchester M13 9PT, England, UK
[2]Science and Technology Facilities Council, Rutherford Appleton Laboratory, Harwell Science and Innovation Campus, Didcot, Oxfordshire OX11 0QX, England, UK

Integrins undergo global conformational changes that specify their activation state. Current models portray the inactive receptor in a bent conformation that upon activation converts to a fully extended form in which the integrin subunit leg regions are separated to enable ligand binding and subsequent signaling. To test the applicability of this model in adherent cells, we used a fluorescent resonance energy transfer (FRET)–based approach, in combination with engineered integrin mutants and monoclonal antibody reporters, to image integrin α5β1 conformation. We find that restricting leg separation causes the integrin to adopt a bent conformation that is unable to respond to agonists and mediate cell spreading. By measuring FRET between labeled α5β1 and the cell membrane, we find extended receptors are enriched in focal adhesions compared with adjacent regions of the plasma membrane. These results demonstrate definitely that major quaternary rearrangements of β1-integrin subunits occur in adherent cells and that conversion from a bent to extended form takes place at focal adhesions.

Introduction

Integrins are heterodimeric transmembrane cell surface receptors that mediate connections between cells or between cells and the ECM (Hynes, 2002). Integrins control many fundamental aspects of cell behavior through their ability to transduce signals bidirectionally across the cell membrane. This transfer is manifested in global conformational changes that specify the activation state and ligand-binding affinity of the receptor. Currently three separate integrin conformational classes have been identified: inactive, active (or primed), and ligand bound, and it is has been proposed that these states correspond to a bent conformation (seen in crystal structures; Xiong, et al., 2001; Zhu et al., 2008), an extended form with a closed headpiece, and an extended form with an open headpiece, respectively (Takagi et al., 2002).

The opening of the headpiece is predicted to induce separation of the integrin subunit legs that allows intracellular signaling molecules to bind during the process of outside-in signaling (Mould et al., 2003a,b; Xiao et al., 2004; Puklin-Faucher et al., 2006). Although there are many images that show the extracellular domains of integrins with splayed legs (Takagi et al., 2002; Nishida, et al., 2006), information regarding the extent to which this occurs in vivo is more sparse and limited to integrins on nonadherent cells (Kim et al., 2003; Partridge, et al., 2005; Lefort et al., 2009).

There is also accumulating evidence to suggest that integrin need not be fully extended to bind ligand. This includes structural (Adair et al., 2005) and biochemical data (Calzada et al., 2002), as well as biophysical fluorescent resonance energy transfer (FRET) measurements that have attempted to measure conformational changes on the cell surface in response to different agonists (Chigaev et al., 2003, 2007; Coutinho et al., 2007). These experiments suggest a level of complexity in integrin conformational changes not revealed by the structural snapshots so far obtained and pose further questions as to exactly how integrin conformation relates to function and how these changes are coupled.

In addition, the vast majority of structural and modeling data have been obtained using constructs of β2 (Beglova et al., 2002; Shi et al., 2007) and β3 (Iwasaki et al., 2005; Rocco et al., 2008) integrins whose activity has to be strictly controlled in vivo and that are mainly expressed on nonadherent cells such as leukocytes and platelets. Therefore, it is still not known whether similar conformational changes apply to all integrin families;

Correspondence to Martin J. Humphries: martin.humphries@manchester.ac.uk

Abbreviations used in this paper: 50K, recombinant fragment of fibronectin comprising type III repeats 6–10; βTD, β-tail domain; DTT, dithiothreitol; FA, focal adhesion; FLIM, fluorescence lifetime imaging microscopy; FN, fibronectin; FRET, fluorescent resonance energy transfer; HFF, human foreskin fibroblast; I-EGF, integrin-EGF; LT, locked together; MFI, mean fluorescence intensity; WT, wild type.

The Rockefeller University Press $30.00
J. Cell Biol. Vol. 188 No. 6 891–903
www.jcb.org/cgi/doi/10.1083/jcb.200907174

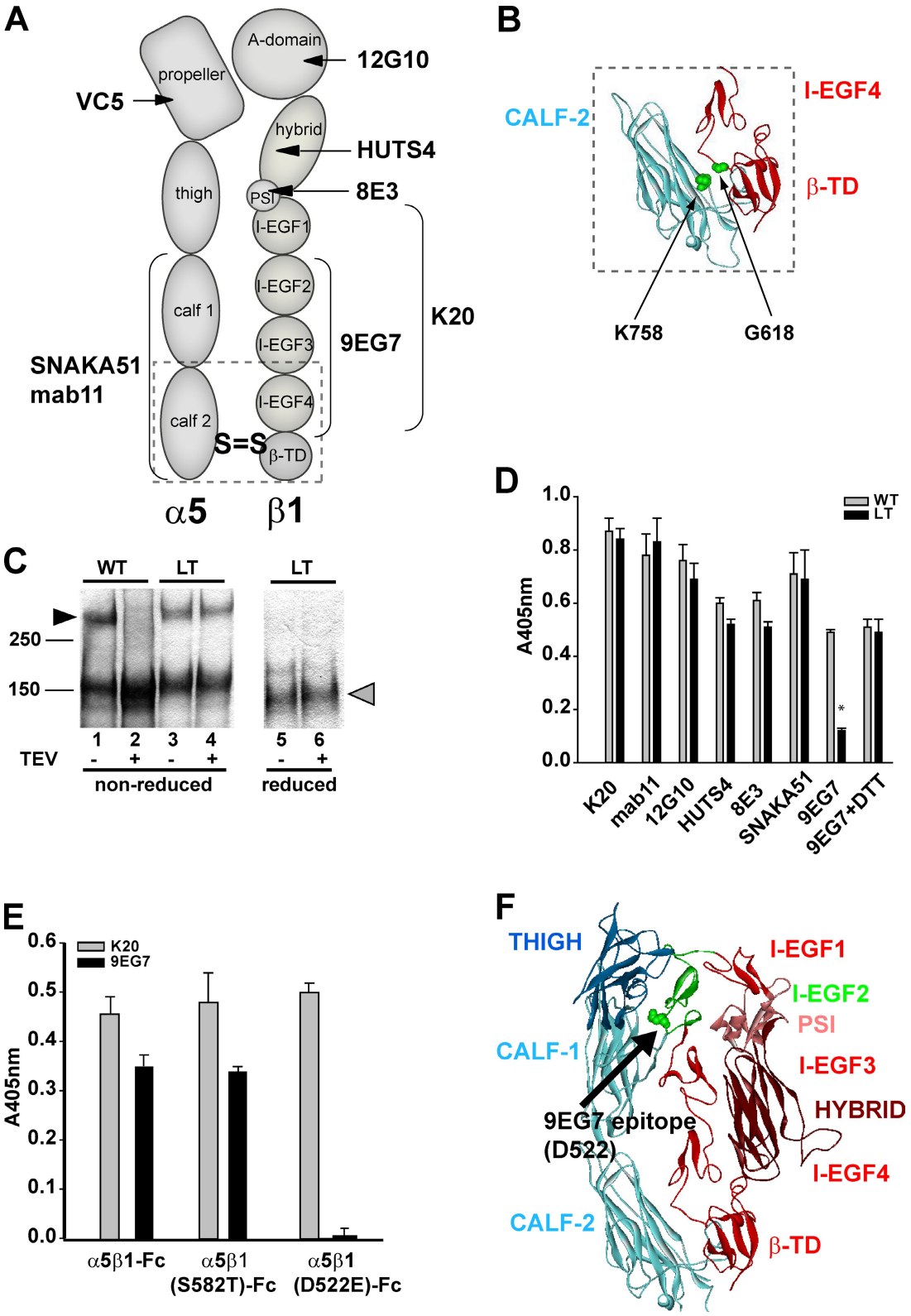

Figure 1. **Preventing leg separation at the calf-2/βTD interface of soluble α5β1-Fc induces bending of the molecule.** (A) Diagram showing the approximate location of the epitopes of the anti-α5 and -β1 antibodies used in this study. The reagents include the activating anti-β1 mAbs 12G10 (βA domain; Mould et al., 1995), HUTS4 (hybrid domain; Mould et al., 2003a), 8E3 (PSI domain; Mould et al., 2005), 9EG7 (I-EGF2-4; Bazzoni et al., 1995), and the activating anti-α5 SNAKA51 (calf1-calf2; Clark et al., 2005). The nonfunction perturbing anti-β1 K20 (I-EGF region; Amiot et al., 1986) and anti-α5 mAb11 (calf1-calf2; LaFlamme et al., 1992) and VC5 (β-propeller; Tran Van Nhieu and Isberg, 1993) are also highlighted. The approximate location of the engineered inter-subunit disulphide bond is indicated. (B) Homology model of α5β1 in the region defined by dotted lines in A. The homology model was built based on an alignment against the αIIbβ3 crystal structure (PDB 3FCS; Zhu et al., 2008), using the same procedures as described previously (Mould et al., 2002). The α5 calf-2 domain is in blue and I-EGF4 and βTD of the β1 subunit are in red. The residues selected for mutation to cysteine to

indeed, there is a striking paucity of conformational information for the ubiquitously expressed β1-integrins that are subjected to greater tensions when mediating cell–ECM adhesion, but whose activity is less likely to be rigidly modulated.

In this study, we have used a variety of approaches to investigate conformational changes in the fibronectin (FN) receptor α5β1. We found that restricting leg separation with an inter-subunit disulphide bond caused the integrin to adopt a bent conformation that was unable to respond to agonists due to a concomitant reduction of movements in the β-subunit leg that accompany receptor activation. Cells expressing this mutated integrin were unable to spread and form focal adhesions (FAs) on FN. Using fluorescence lifetime imaging microscopy (FLIM)–based FRET analysis, we found that wild-type (WT) α5β1 in the FA of cells spread on FN was in an extended form compared with unligated receptor. These results extend our understanding of integrin structure–function relationships to β1-integrins on adherent cells and underscore the importance of integrin extension and leg separation in vivo.

Results

Preventing leg separation at the calf-2/βTD interface of soluble α5β1-Fc induces bending of the molecule

Conversion of an integrin from an inactive to a ligand-bound state is predicted to involve a separation of the leg regions of the receptor (Zhu et al., 2007). To examine the importance of leg separation to the function of the FN receptor α5β1, we used a previously described, recombinant-soluble α5β1-Fc fusion protein (Coe et al., 2001) to engineer a construct in which the membrane-proximal α5β1 calf-2/β-tail domain (βTD) interface was constrained by introduction of a disulphide bond between the α- and β-subunits to form a potential locked-together (LT) integrin (Fig. 1, A and B). Lysine-758 in the calf-2 region of α5-Fc, and glycine-618 in the βTD of β1-Fc were chosen for mutation as they are the equivalent residues to those introduced in αvβ3 to produce a similarly constrained receptor (Kamata et al., 2005). Successful production of the LT protein was confirmed by SDS-PAGE after removal of the Fc domain from the β1-subunit (Fig. 1 C).

A panel of stimulatory anti-α5 and -β1 monoclonal antibodies (mAbs), with epitopes spanning the entire integrin extracellular domain, was used to examine the conformation of the mutated receptor. All the antibodies tested bound equally well to WT and LT α5β1-Fc with the exception of the anti-β1 mAb 9EG7 (Fig. 1 D). Antibody binding was restored upon treatment with dithiothreitol (DTT), confirming that the epitope had not been compromised by the mutation. These data indicate that restraining the integrin legs induces a conformation of α5β1-Fc that masks the 9EG7 epitope. The binding site for 9EG7 lies within the integrin-EGF (I-EGF)–like repeats 2–4 of β1 (Bazzoni et al., 1995), but to assess the effect on integrin conformation more precisely, mutations were performed in WT β1-Fc to pinpoint the precise epitope. 9EG7 was raised against mouse β1 in a rat background but cross-reacts with the human molecule (Lenter et al., 1993); therefore, residues that were the same in human and mouse β1 but different to rat within I-EGF 2–4 were selected for mutation. Only two residues fulfilled these criteria, D522 and S582 in the human molecule. These residues were mutated to the corresponding residues of the rat sequence (glutamate and threonine, respectively) in human β1-Fc, expressed with α5-Fc, and tested for binding of 9EG7 in Fc-capture ELISA. D522E totally abolished 9EG7 binding, whereas S582T had no effect (Fig. 1 E). Thus, the epitope for 9EG7 was pinpointed to D522 in I-EGF-2 of the β1-subunit.

A homology model of α5β1 revealed that D522 is located in the genu or knee region of the molecule, shielded by the α-subunit on one side and the β-subunit on the other when the receptor is in a bent conformation, making it inaccessible to the antibody (Fig. 1 F). Therefore, we infer that restraining the legs of α5β1-Fc at the calf-2/βTD interface causes the integrin to adopt a bent conformation that masks the 9EG7 epitope, and that binding of this antibody therefore reports the extended conformations of β1-integrins. Currently, there are no structural data and very limited biochemical evidence to indicate bending in β1-integrins (Mould et al., 2005); however, the data obtained with 9EG7 strongly suggest that α5β1 can adopt a bent conformation if the membrane-proximal extracellular interface is held in close association.

Restraining leg separation of soluble α5β1-Fc at the calf-2/βTD interface impairs ligand binding and abrogates the ability of activating antibodies to stimulate ligand binding

As the bent conformation of integrins is generally accepted to have low affinity for ligand, the effect of restraining the legs of α5β1 on ligand binding was studied using a 50-kD recombinant

form the inter-subunit disulphide bond, Lys758 in α5 and Gly618 in β1, are shown in CPK form in green. (C) WT or LT α5β1-Fc was purified from culture supernatant and then incubated with Tobacco Etch Virus protease (TEV) to remove the Fc domain from the β-subunit. 3–8% SDS-PAGE gel showing α5β1-Fc dimer (black arrowhead, M_r ~300 kD) that dissociates upon TEV protease treatment in WT (lane 2) but not LT (lane 4) integrin. Reduction of the disulphide bond separates LT into its two subunits (gray arrowhead, α5-Fc M_r ~145 kD, β1-Fc ~140 kD). The band at 150 kD in nonreduced samples is contaminating bovine Ig from culture medium. This dissociates upon reduction into its component 50- and 25-kD subunits not included in the figure. Numbers to the left of the gel indicate the position of M_r markers. (D) WT or LT α5β1-Fc was captured onto anti–human Fc-coated ELISA plates and the binding of activating anti-α5 (SNAKA51) and anti-β1 (12G10, HUTS4, 8E3, and 9EG7) antibodies to WT (gray bars) and LT (black bars) α5β1-Fc compared with nonfunction perturbing anti-α5 (mAb11) and anti-β1 (K20) in the presence of 1 mM each of Ca^{2+} and Mg^{2+}. DTT was included at 250 μM where indicated. Error bars show ±SD of three separate experiments. (*, P = 0.001; *t* test). (E) Binding of K20 (gray bars) or 9EG7 (black bars) to WT α5β1-Fc, α5β1(S582T)-Fc, and α5β1(D522E)-Fc. Error bars indicate ±SD of three separate experiments. (F) Homology model of extracellular domain of α5β1 showing the position of the 9EG7 epitope at D522 in I-EGF2, which is colored green with D522 represented in CPK form. For clarity, the integrin headpiece (α5 β-propeller and βA domain) is not included. The model was prepared as in panel B.

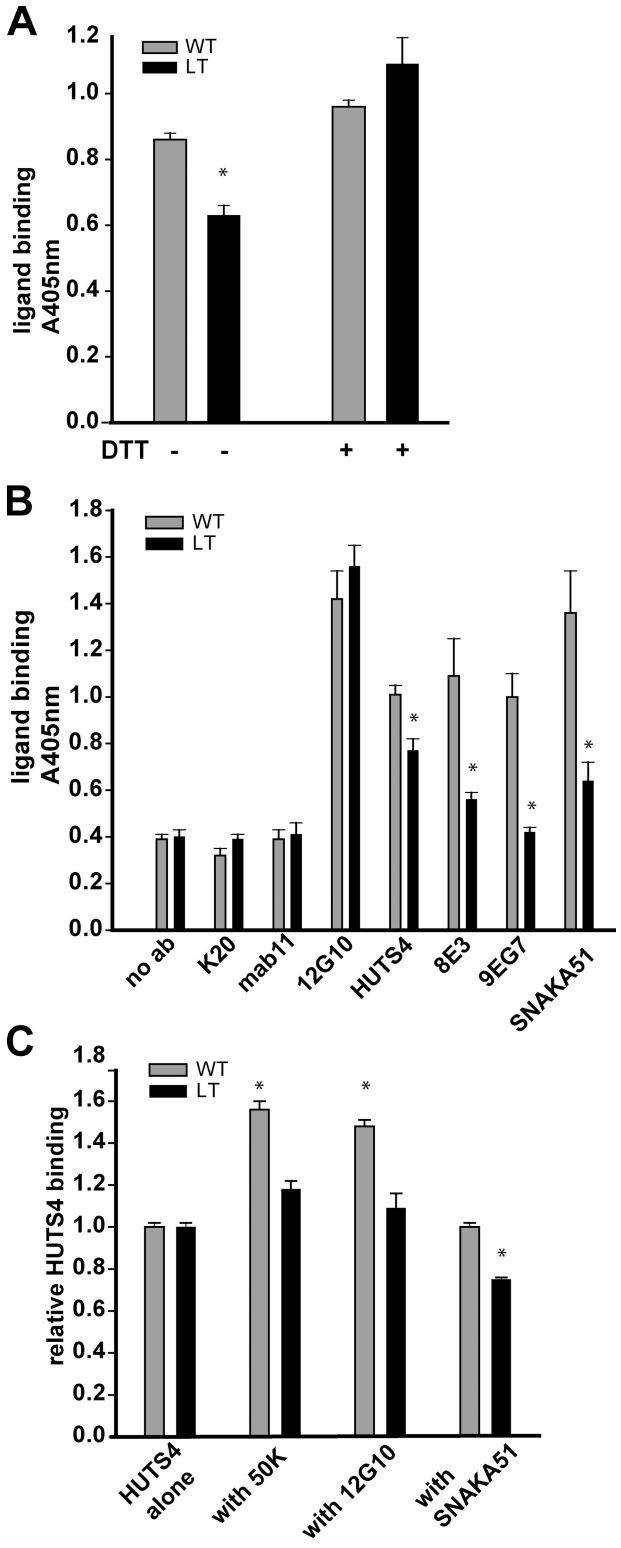

Figure 2. **Restraining leg separation of soluble α5β1-Fc at the calf-2/βTD interface impairs ligand binding and abrogates the ability of activating antibodies to stimulate ligand binding.** (A) Fc-capture ELISA showing binding of FN fragment (type III repeats 6–10; 50K) to WT (gray bars) and LT α5β1-Fc (black bars) before and after treatment with 250 µM DTT in the presence of 1mM Mn^{2+}. (B) Fc-capture ELISA showing binding of 50K to WT (gray bars) and LT (black bars) α5β1-Fc together with activating anti-α5 (SNAKA51) and anti-β1 (12G10, HUTS4, 8E3, and 9EG7) antibodies, compared with nonfunction-perturbing anti-α5 (mAb11) and anti-β1 (K20) in the presence of 1 mM each of Ca^{2+} and Mg^{2+} (*, P = 0.001; *t* test). (C) Fc-capture ELISA showing the effects of various α5β1 agonists on the binding of HUTS4 to WT and LT α5β1-Fc. Error bars indicate ±SD for three separate experiments. *, P < 0.001; *t* test.

fragment of FN comprising type III repeats 6–10 (50K). Neither WT nor LT α5β1-Fc bound ligand in the presence of Ca^{2+} and Mg^{2+} (Fig. 2 B). However, in the presence of Mn^{2+}, WT α5β1-Fc exhibited high ligand binding that was significantly reduced (P < 0.001) but not completely abolished in the LT receptor (Fig. 2 A). Treatment with DTT fully restored ligand binding capability.

Activating anti-integrin antibodies exert their effect by inducing or stabilizing an active conformer to increase ligand binding (Humphries, 2004). The effect of restraining the legs on ligand binding in the presence of stimulatory mAbs was therefore studied to investigate how conformational changes leading from inactive to active receptor are coupled. These experiments were performed in the presence of Ca^{2+} and Mg^{2+} where constitutive ligand binding is low, thus allowing the full activating effect of the antibodies to be observed. The nonfunction-perturbing mAbs K20 (β1) and mAb11 (α5) had no effect on ligand binding to either the WT or LT construct and, as expected, the stimulatory anti-β1 (12G10, HUTS4, 8E3, and 9EG7) and anti-α5 (SNAKA51) mAbs all enhanced ligand binding to the WT α5β1-Fc (Fig. 2 B). However, clear differences were apparent in the ability of the antibodies to augment 50K binding to LT α5β1-Fc. The function of 12G10 was not impaired, but HUTS4, 8E3, and 9EG7 showed a decreased ability to enhance 50K binding that correlated with the distance of their epitopes from the disulphide bond between the α- and β-subunit (Fig. 1 A). In addition, the ability of SNAKA51, the epitope for which lies in the α5 calf-1/calf-2 domain (Clark et al., 2005), to stimulate 50K binding to LT α5β1-Fc was also markedly reduced. These results demonstrate that the formation of a disulphide lock between the α5 calf domain and the β1 βTD compromised induction of the related allosteric shape changes that equate to the high affinity ligand-bound conformation. Thus, these changes are dependent on integrin leg separation.

An outward movement of the hybrid domain, producing the open integrin headpiece, is a hallmark of high affinity integrin and is reported in β1-integrins by the HUTS4 antibody that binds to the inner face of the domain (Mould et al., 2003a). The above results suggest that restraining integrin leg movement results in a reduced ability of this region to take on its high affinity, open position. To gain further information on shape changes in the LT receptor, the effects of various agonists such as ligand (50K), and the stimulatory antibodies 12G10 (anti-β1) and SNAKA51 (anti-α5), on the binding of HUTS4 to WT and LT α5β1-Fc were examined. Both 50K and 12G10 caused an increase in the binding of HUTS4 to WT α5β1-Fc that was almost completely abrogated in the LT integrin (Fig. 2 C), suggesting that restraining leg separation reduces hybrid swing-out. This result further implies that leg separation is directly coupled to hybrid domain movement.

In contrast, binding of SNAKA51 was unable to stimulate HUTS4 binding in the WT integrin (Fig. 2 C). This would

Table I. **Flow cytometry analysis of integrin conformation**

Integrin subunit	Antibody	MFI		
		$CaMg^{2+}$	Mn^{2+}	Mn^{2+} + 50K
β1	K20[a]	143.87	138.17	141.56
	12G10	59.49	102.35	95.81
	HUTS4	4.85	19.04	26.94
	8E3	5.48	6.24	6.86
	9EG7	34.33	61.02	74.30
α5	mab11[a]	25.28	26.83	23.42
	SNAKA51	3.24	6.21	12.68

Flow cytometry was used to measure the binding of anti-α5β1 antibodies to HFF cells under conditions promoting low (in the presence of 1 mM each Ca^{2+} and Mg^{2+}) and high affinity (in the presence of Mn^{2+} with or without the addition of 50K ligand). The non-function perturbing antibodies K20 (anti-β1) and mAb11 (anti-α5) were used to estimate total expression of each subunit. The results are expressed as mean fluorescence intensity (MFI) with background binding levels of normal rat or mouse IgG subtracted, and are representative of three separate experiments.

[a]Neutral antibody.

suggest that SNAKA51 exerts its stimulatory effect, at least on the soluble, recombinant α5β1-Fc, by inducing a destabilization of the leg regions that is not sufficient to induce hybrid swing-out. Surprisingly, in the LT construct, SNAKA51 appeared to inhibit the binding of HUTS4, lending weight to the hypothesis that the LT integrin is bent, because only in this conformation would the epitopes of these antibodies be close enough to affect each other's binding. Taken together, these results indicate that restraining the integrin legs inhibits the effect of agonists and interferes with structural rearrangements associated with the switch from inactive to active receptor. Therefore, leg separation and hybrid movement are intimately associated.

Epitope expression on cell surface integrin

A series of experiments were then conducted to extend the findings obtained with soluble receptors to those expressed at the cell surface. Using flow cytometry, the level of binding of activating anti-α5 and anti-β1 antibodies was used to assess α5β1 conformation on the cell surface of human foreskin fibroblasts (HFFs) under conditions promoting low (in the presence of Ca^{2+} and Mg^{2+}) and high (in Mn^{2+} with or without 50K) affinity integrin (Table I). The binding of 9EG7 to resting cells was significantly above background levels (mean fluorescence intensity [MFI] 34.33), indicating the presence of primed β1-integrin on the cell surface.

The binding of SNAKA51 was low, but increased significantly with the addition of Mn^{2+} and ligand (MFI from 3.24 to 12.68), indicating that this antibody preferentially binds to the ligand-bound form of the integrin and is consistent with the idea that a conformational change in the leg regions, which may involve leg separation, induced by ligand increases the exposure of the SNAKA51 epitope. Therefore, we conclude that SNAKA51 binds to a ligand-bound conformer in which the integrin legs are most likely separated and that SNAKA51 activates integrin by stabilizing a conformer that is competent to bind ligand.

FLIM-based FRET analysis of conformation differences of integrin α5β1 in HFF cells spread on FN

Having surveyed the conformation of α5β1 on cells in suspension, we next examined how integrin conformation is affected when cells spread and force is generated on the integrin–ligand complex at sites of adhesion complex formation. To address how integrin conformation varies with location, and in particular to assess the degree of extension of α5β1 present in adhesion complexes in comparison to adjacent regions of the cell membrane, whole cells were imaged using time-correlated single photon counting (TCSPC) FLIM-based FRET analysis. FRET is a phenomenon by which the excited-state energy of an optically excited molecule (donor) is transferred to a neighboring molecule (acceptor) nonradiatively via intermolecular dipole coupling (Lakowicz, 1983). FRET is therefore extremely sensitive to short intermolecular distances (<10 nm), with the efficiency of FRET varying as the inverse sixth power with distance (Stryer and Haugland, 1967). TCSPC-FLIM-FRET directly measures the time between the absorption and emission of individual photons in the FRET donor fluorophores and has the advantage of providing quantitative results largely free from artifacts such as photobleaching and radiative transfer (Martin-Fernandez et al., 2002).

The α5β1 headpiece on HFF cells was labeled with an Alexa Fluor 546–tagged Fab fragment of a nonfunction perturbing anti-α5 mAb VC5 and the cell membrane stained with C_{18}DiD. An overlap between the emission spectrum of Alexa 546 and the absorption spectrum of C_{18}DiD allows these two dyes to act as a FRET pair. A shortening of the donor (VC5-Fab-Alexa 546) lifetime from that observed in the absence of acceptor (C_{18}DiD) was used to quantify FRET between the two fluorophores. To eliminate the possibility that rigidity in the orientation of the dye molecules could account for any variations in FRET efficiencies, the steady-state fluorescence anisotropy of C_{18}DiD in lipid vesicles was measured. This was found to be 0.154, whereas the maximum possible value expected for static dye molecules is 0.4 (Lakowicz, 1983), indicating that the acceptors used were free to rotate and sample a large number of orientations within the lifetime of the donor. Therefore, the measured FRET efficiencies depended only upon the donor and acceptor separation distance and the density of acceptors in the membrane (Stryer and Haugland, 1967; Haas et al., 1978).

The donor (VC5-Fab-Alexa 546) was found to label both membrane and adhesion complexes in cells expressing both WT and LT α5β1 equally, showing that the access of the Fab to its

epitope is not dependent on the conformation of the integrin receptor (Fig. S1 A). In the absence of acceptor, the mean fluorescence donor lifetime was 2,588 ± 183 picoseconds (ps; mean ± SD) within adhesion complexes and 2,505 ± 220 ps in the rest of the cell membrane (Fig. 3, D and F). The C_{18}DiD was found to label HFF cell membranes uniformly within the areas of measurement (Figs. 3 E and Fig. S1 B), indicating that clustering of the integrin receptors did not interfere with the distribution of the acceptor. The density of acceptor in the cell membrane of the cell illustrated in Fig. 3 E was calculated to be 0.937 acceptors per unit area (R_0^2) and in the presence of acceptor, the donor lifetime was reduced to 1,779 ± 190 ps within adhesion complexes and to 1,198 ± 127 ps in the adjacent cell membrane (Fig. 3, A, C, and F). This finding is indicative of a lower efficiency of FRET at the same acceptor density, and therefore a greater distance between the donor-labeled integrin headpiece and the acceptor-labeled cell membrane. Assuming that the VC5-Fab-Alexa 546 adopts the same orientation relative to integrin molecules inside and outside of adhesion complexes, this infers that the integrin molecules were in a more extended conformation inside adhesion complexes.

As stated above, FRET efficiency can vary with acceptor concentration due to the different numbers of acceptors available to the donors as FRET partners; therefore, similar measurements were made over several cells with a range of acceptor densities and a consistent difference was found between the FRET efficiency adjacent to and within adhesion complexes (Fig. 3 G). These results indicate that there is decreased FRET efficiency between donor and acceptor within adhesion complexes and demonstrates that α5β1 in these complexes is in a more extended form than that in the adjacent plasma membrane.

To eliminate the possibility that the lower FRET efficiencies observed in adhesion complexes were due to an artifact arising from a higher concentration of donor molecules that could compete with each other for the available acceptors, two separate control experiments were performed. Initially, the Alexa 546 fluorescence was reduced by photobleaching before measuring lifetimes. This had no effect on the difference in lifetimes seen within and outside adhesion complexes (Fig. S2 A). To confirm this observation, cells were labeled with VC5-Fab-Alexa 546 together with increasing proportions of unlabeled VC5-Fab fragments to reduce the number of fluorescent donor molecules available for FRET. Again, no significant effect on lifetimes was observed (Fig. S2 B). We therefore conclude that the decreased FRET efficiency observed between the molecules in adhesion complexes was due to an increased average separation between donor and acceptor. These results provide strong evidence that ligand-bound α5β1 adopts an extended conformation compared with unligated receptor.

Restraining leg separation perturbs α5β1 function in vivo

The experiments using soluble integrin in Figs. 1 and 2 indicate that restraining the legs of soluble α5β1-Fc affects its conformation and activity. To examine the effect of restraining the legs on the function of this integrin in a cellular context, both WT and LT full-length α5β1 were expressed in β1-null GD25 cells (Wennerberg et al., 1996). To facilitate visualization of each subunit, α5 was tagged with CFP and β1 with YFP at their C termini. Western blot analysis confirmed formation of the LT integrin, which dissociated upon reduction into its component subunits (Fig. 4 A).

Flow cytometric analysis was first performed to assess the expression of LT and WT α5β1 on the cell surface. Both receptors were expressed to a similar degree, as measured by almost equal levels of K20 binding (Fig. S3; MFI 105.78 for WT and 108.89 for LT). Binding of 9EG7, however, was significantly reduced in cells expressing LT integrin compared with WT (MFI 6.95 and 31.92, respectively), but this was restored after treatment of the cells with 250 µM DTT (MFI 25.42). These results confirm that LT α5β1 was expressed on the cell surface in a bent conformation.

Cells expressing WT α5CFPβ1YFP spread and produced well-formed adhesion complexes on FN that were 9EG7 positive, indicating a high affinity, extended state. Cells expressing LT α5CFPβ1YFP also spread and produced clusters of β1 that were less well formed than WT and had a significantly smaller mean area (7.73 ± 3.69 µm^2 compared with 14.86 ± 9.64 µm^2 for cells expressing WT α5β1; $P < 0.001$; Fig. 4 B). Importantly, these clusters had significantly reduced binding of 9EG7 (Fig. 4 C), suggesting that, as with soluble α5β1, preventing leg separation caused the integrin to adopt a bent conformation that could nevertheless be directed into clusters on the cell surface. Treatment of the LT α5β1-expressing cells during spreading with DTT restored 9EG7 staining (Fig. 4 B).

The same cells were co-stained with SNAKA51 to detect the ligand-bound conformation of α5β1 and quantitative analysis of the fluorescence intensity of α5CFP, β1YFP, and SNAKA51 staining performed. The intensity profile across adhesion complexes for cells transfected with WT α5β1 (Fig. 4 D) revealed an increase in intensity in all three channels representing α5CFP, β1YFP, and SNAKA51. This indicates that the WT integrin is in an extended, ligand-bound conformation in which the integrin legs are likely to be separated. In contrast, while there was a clear increase in intensity in α5CFP and β1YFP over the integrin clusters in the cells expressing LT integrin, the staining intensity for SNAKA51 was very low. Quantitation of the ratio of SNAKA51 to total α5CFP intensities showed a highly significant decrease in SNAKA51 binding in the LT receptor (Fig. 4 E) which, like 9EG7 staining, was restored upon addition of DTT. These results confirm that the LT α5CFPβ1YFP is in an inactive, nonligand-bound state but is still able to form clusters in the cell.

GD25 cells express endogenous mouse α5, which could be available to pair with the transfected human β1. Immunocytochemical analysis with a mouse-specific anti-α5 antibody showed some colocalization of mouse α5 with β1YFP in these clusters (Fig. S4 A), but because 9EG7 staining remained low, it is likely that it had little effect on the results obtained. However, to eliminate any contribution from mouse integrins, GD25 cells expressing WT or LT α5β1 were plated onto a human α5β1-specific ligand, the cyclic peptide-IgG conjugate CRRETAWAC-IgG (Humphries et al., 2000). Although CRRETAWAC-IgG is a much less potent ligand than FN (Fig. S4 B), 12% (±1%) of

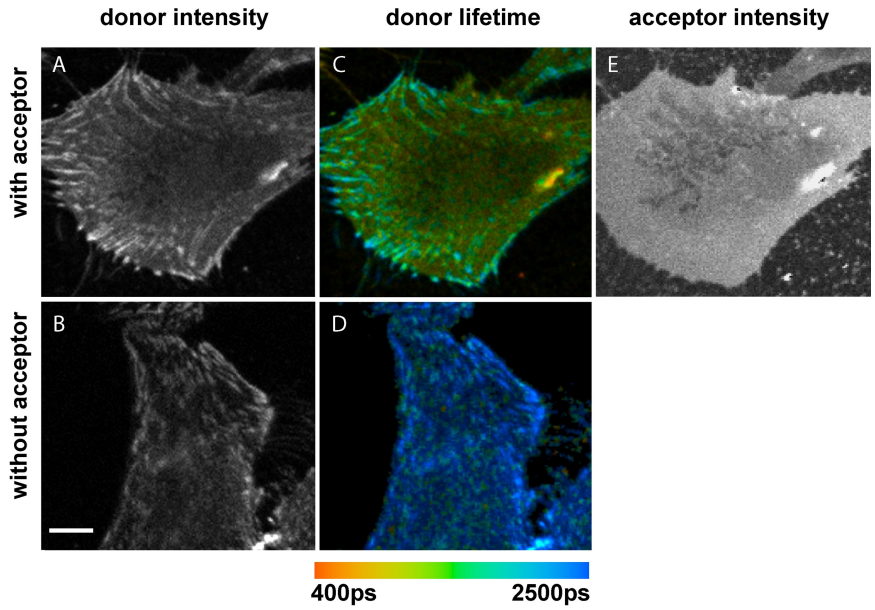

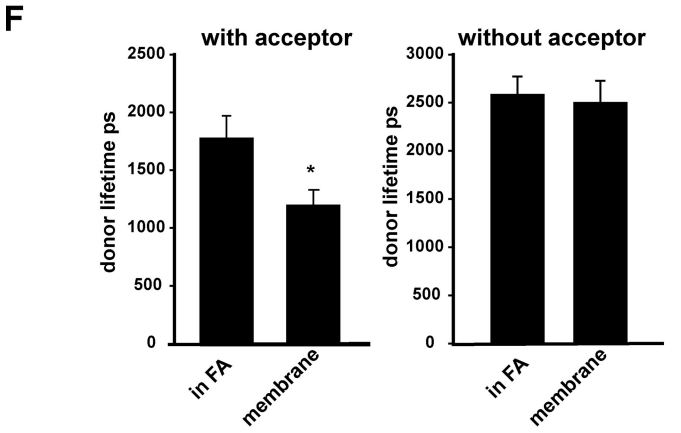

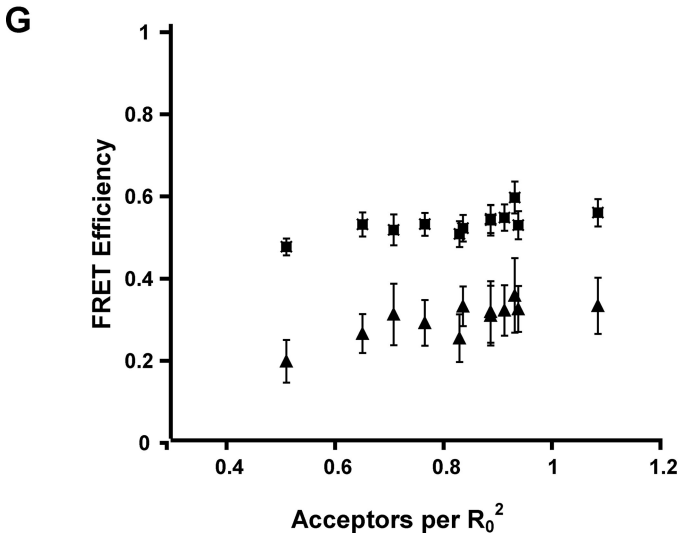

Figure 3. **TCSPC-FLIM–based FRET analysis of conformation differences of integrin α5β1 in HFF cells spread on FN.** Representative HFF cells spread on FN and stained with Alexa 546-VC5-Fab fragment (the donor, panels A and B) either with (top row) or without (bottom row) fluorescent membrane stain DiD (the acceptor). C and D show false-colored FLIM images representing donor fluorescence lifetimes from individual pixels. Short lifetimes are located toward the red end and long lifetimes toward the blue end of the spectrum. (E) DiD staining. (F) Average lifetimes (in picoseconds; ps) of Alexa 546 fluorescence measured in adhesions complexes (FA) and in areas between adhesion complexes in the cell membrane of the cells illustrated in A and B. n = 50 measurements each from each cell, error bars indicate ±SD (*, $P < 0.001$; t test). (G) Graph showing FRET efficiencies over a range of acceptor densities in different cells within adhesion complexes (triangles) and in the adjacent cell membrane (squares). n = >20 measurements from each of 12 cells. Error bars indicate ±SD.

GD25 cells expressing WTα5β1 formed adhesion complexes that were both 9EG7 and SNAKA51 positive. In contrast, cells expressing LT α5β1 not only did not form adhesion complexes, but also failed to spread properly on the peptide ligand (cell area = 623 ± 121 μm^2 compared with 1,448 ± 458 μm^2 for cells expressing WT receptor; $P < 0.001$; Fig. 5). This result demonstrates that restraining integrin α5β1 subunit separation on the cell surface abrogates cell spreading and severely disrupts integrin function. Therefore, cell spreading and adhesion complex formation in adherent cells requires α5β1-integrin to be in an extended conformation and one in which leg movement can occur.

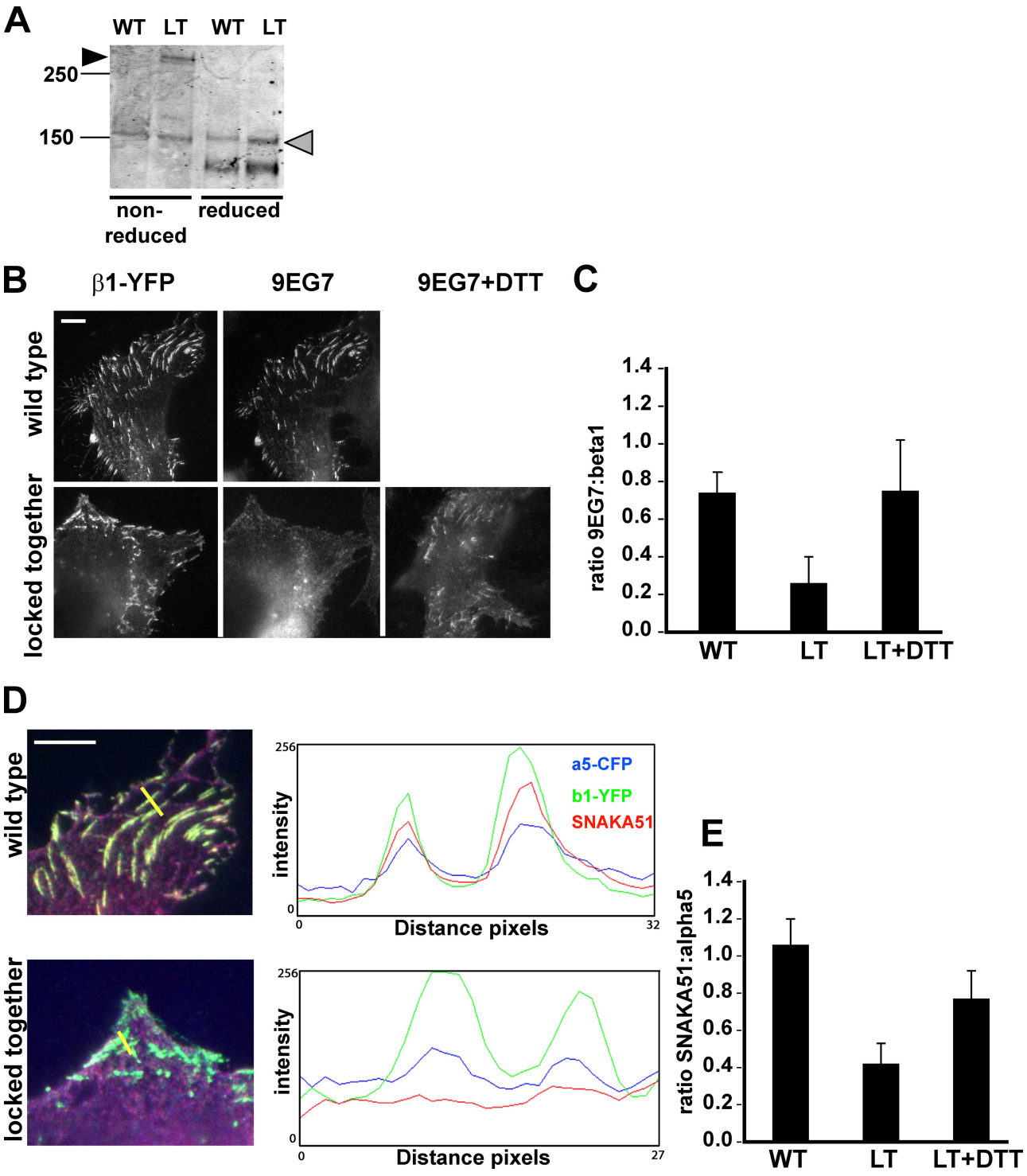

Figure 4. **Restraining leg separation perturbs α5β1 function in vivo.** (A) β1-integrin was immunoprecipitated from lysates of GD25 cells expressing either WT or LT α5CFPβ1YFP 24 h after transfection, followed by immunoblotting for integrin α5 (antibody H-104; Santa Cruz Biotechnology, Inc.). Black arrowhead indicates a 300-kD band corresponding to LT integrin, which dissociates upon reduction into component subunits (gray arrowhead). Numbers to the left of the gel indicate position of M_r markers. (B) GD25 cells expressing WT or LT α5CFPβ1YFP co-stained with 9EG7-Alexa 647 to detect active integrin. Cells were treated with 1 mM DTT during spreading where indicated. Bar, 10 µm. (C) Quantification of the ratio of fluorescence intensities of 9EG7 staining to total β1YFP in β1-integrin clusters. *n* = fluorescence intensity measurements of 100 clusters from at least 10 cells for each condition. Error bars indicate ±SD. (D) The same cells were co-stained with SNAKA51-Alexa 555 to detect ligand-bound α5β1. The fluorescence intensity profiles depict the area of the yellow line drawn in image overlays and compare the fluorescence intensities of total β1 (β1-YFP; green), total α5 (α5-CFP; blue), and SNAKA51 (red). (E) Quantification of the ratio of fluorescence intensities of SNAKA51 staining to total α5-CFP in β1-integrin clusters. *n* = fluorescence intensity measurements of 100 clusters from at least 10 cells for each condition. Error bars indicate ±SD. Bar, 10 µm.

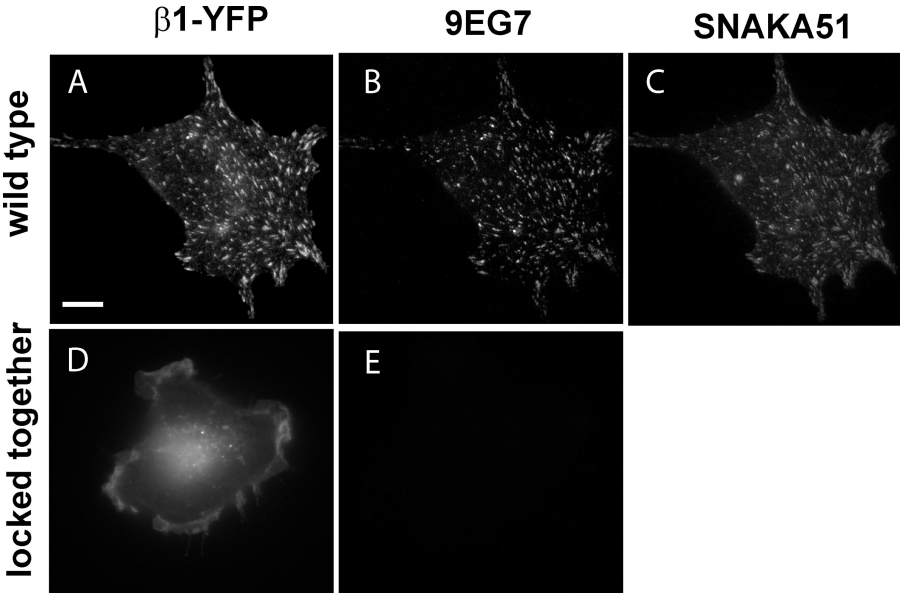

Figure 5. **Spreading of GD25 cells expressing WT or LT α5β1 on CRRETAWAC-IgG.** GD25 cells transiently expressing either WT or LT α5CFPβ1YFP were allowed to spread on CRRETAWAC-IgG for 60 min, fixed, and stained with 9EG7-Alexa 647 and SNAKA51-Alexa 555. (A and D) β1-YFP fluorescence; (B and E) 9EG7 staining; (C) SNAKA51 staining. Bar, 10 μm.

Discussion

The results of this study have extended the current model of conformational changes in integrin activation to include β1-integrins on adherent cells. Our results provide strong evidence that a close interaction of the membrane-proximal extracellular domains is necessary to maintain the receptor in a low affinity state. Once ligated to ligand and clustered in adhesion complexes, the integrin is in an extended conformation where the legs are separated. Integrin in which leg movement is constrained cannot mediate efficient cell spreading.

An important finding of this study was to pinpoint the 9EG7 epitope to aspartate 522 in I-EGF-2 located in the knee region of the β-subunit. The epitope of 9EG7 mimics almost exactly that of the anti-β2 mAb KIM127, which incorporates residues 504–508 of the β2-subunit (Lu et al., 2001). KIM127 has been proven through structural studies to report an integrin extension event that correlates with activation (Beglova et al., 2002; Shi et al., 2007). Therefore, we conclude that binding of 9EG7 similarly reports extended conformations of β1-integrins and binding of this antibody stabilizes an active form of the receptor.

Cell-based flow cytometry assays demonstrate that the 9EG7 epitope is exposed on unstimulated HFF cells, which implies a degree of spontaneous β1 extension. This finding is in contrast to KIM127, whose binding to leukocytes is very low in the absence of stimulation by agonists (Lu et al., 2001). In turn, this suggests a less rigid control of the activity of the β1-integrins, which may be a reflection of their role as mediators of steady-state cell–ECM binding, compared with the β2 and β3 receptors that need to exhibit a rapid response to injury from their default inactive state (Shattil et al., 1998). However, this may not necessarily be reflected across all cell types. Specific cellular functions may dictate the control of integrin conformational changes, particularly as different ligands appear to induce diverse conformers of β1-integrin heterodimers (Bazzoni et al., 1998).

The data for mAb and ligand binding to the recombinant α5β1-Fc compared with cell-based measurements exhibited some degree of incongruity, which is a reflection of the disparity of the two experimental systems. The Fc domain of the integrin fusion protein constructs includes 14 residues of the upper hinge and hinge regions of the human γ1 constant domains (Ridgway et al., 1996), which may introduce a degree of flexibility in these constructs that is not seen on cellular integrin. It is likely that the epitopes for the mAbs tested are much more accessible in the recombinant receptor than in whole integrin expressed on the cell surface, and this may have led to apparent differences in their levels of binding (in particular for SNAKA51 and 8E3). In addition, although restricting leg movement had a dramatic effect on cell adhesion, ligand binding to the recombinant construct was less strikingly modulated by the leg constraint. It is possible that even though the LT receptor is bent, the ligand-binding pocket is accessible to the small fragment of FN used in this assay, particularly as the presence of manganese ions could prime the ligand-binding pocket independently of other activation-associated conformational changes.

Our results clearly show that SNAKA51 is a reporter of ligand-bound α5β1 which, on available evidence, adopts a conformation in which the leg regions are apart (Takagi et al., 2002; Kim et al., 2003; Zhu et al., 2007). We therefore infer that this antibody also reports leg separation; an assumption that is supported by our data because binding of SNAKA51 to LT α5β1 expressed on GD25 cells was very low.

Ligand binding is accompanied by an opening of the integrin headpiece by hybrid domain swing-out (Mould et al., 2003a; Xiao et al., 2004). Using recombinant integrin, we have demonstrated that hybrid domain swing-out is directly coupled to leg separation and that prevention of the latter abrogates conformational changes associated with activation and ligand binding. In vivo, destabilization of the integrin transmembrane or cytoplasmic domain association by mutation (Hughes et al., 1996; Luo et al., 2004) or the binding of talin (Wegener et al.,

2007) activates integrin and is likely to facilitate to hybrid movement (Takagi et al., 2001). However, the extent of the contribution of outside-in and inside-out events to integrin conformational changes and particularly hybrid domain movement is difficult to dissect and remains unclear. At present, there is more evidence to suggest that outside-in signaling plays a greater role in this conformational change (Mould et al., 2003b; Takagi et al., 2003; Xiao et al., 2004). However, global shape changes are a result of a fine balance of the equilibrium between protein–integrin binding events on both sides of the cell membrane. In adherent cells, the contribution of forces to the formation and stabilization of specific integrin conformations is an area of increasing interest. There is evidence that application of force can increase the rate of formation and the lifetime of integrin–ligand bonds. Modeling data have predicted this to occur by stabilizing the ligand-bound high affinity conformation (Puklin-Faucher et al., 2006; Zhu et al., 2008), and experimental data have demonstrated strengthening of these interactions by the formation of catch bonds (Friedland et al., 2009; Kong et al., 2009). Previous work using αIIbβ3 has suggested that force is required for receptor extension (Zhu et al., 2008), whereas our results indicate that some degree of spontaneous unbending occurs for α5β1. This apparent contradiction could be a reflection of the diversity of conformational control mechanisms that characterize individual integrin receptors. It remains to be determined whether force is needed to stabilize an extended integrin, but very recent work has indicated that the binding of talin to αIIbβ3 tethered in lipid nanodiscs is sufficient to activate and extend the receptor in the absence of force (Ye et al., 2010). We speculate that for α5β1 the application of force may contribute to the stability of an extended receptor and to facilitate subsequent hybrid domain movement.

Previous studies using integrins with constrained leg movement have been restricted to either soluble constructs (Takagi et al., 2001) or full-length integrin on cells in suspension (Luo et al., 2004; Kamata et al., 2005). By expressing LT α5β1 in GD25 cells, we have been able to gain further insight to the role of conformational changes in adherent cell function. Cells expressing LT α5β1 were unable to form proper FAS, but did appear in clusters on the cell surface if nonconstrained receptor was present. This observation suggests that low affinity integrin could be a component of adhesion complexes. Whether this is true under normal circumstance is not known, and although it can be envisaged that having a pool of readily available inactive receptor might be beneficial to the cell, existing evidence suggests that clustering of integrin only occurs after integrin activation and ligand binding (Kim et al., 2004; Cluzel et al., 2005). It is possible that the LT α5β1, although 9EG7 negative, is sufficiently unbent to bind ligand and therefore cluster, but not to initiate downstream signaling pathways leading to cell spreading, which requires leg separation (Zhu et al., 2007). A very recent study has suggested that αIIbβ3 clusters in response to talin binding without a concomitant increase in the affinity of the integrin (Bunch, 2010), implying that low affinity receptor is a component of some integrin adhesion complexes.

The reduction in the donor fluorescence lifetime in adhesion complexes in the presence of acceptor compared with donor alone may suggest that a proportion of receptor is not fully extended. FRET between fluorophores occurs when they are within a distance of 10 nm and the distance of the integrin headpiece to the membrane in a fully extended receptor is almost double this, implying that lower affinity receptor is present in adhesion complexes. Some studies have attempted to measure absolute distances of the distance between the integrin headpiece and the cell membrane (Chigaev et al., 2003; Coutinho et al., 2007), but at best these provide only an average measurement from across the whole cell. Importantly, the FLIM method used in the present study, while again measuring average FRET efficiencies, allows sampling from different areas within the same cell and provides a more detailed survey of integrin conformations present on the cell surface. The results provide strong evidence that extended α5β1-integrin is enriched in adhesion complexes.

Materials and methods

Antibodies and reagents

Antibodies binding to human β1-integrin were 9EG7 (a gift of D. Westweber, Max Planck Institute for Molecular Biomedicine, Munster, Germany), HUTS4 (Millipore), K20 (Beckman Coulter), 12G10 (Mould et al., 1995), and 8E3 (Mould et al., 2005). Antibodies recognizing human α5 were mAb11 (a gift of K. Yamada, National Institute of Dental and Craniofacial Research, NIH, Bethesda, MD), VC5 (a gift of R. Isberg, Tufts University Medical School, Boston, MA), and SNAKA51 (Clark et al., 2005). Fab fragments of VC5 were produced by ficin cleavage of purified IgG followed by removal of Fc-containing fragments using protein A–Sepharose, according to the manufacturer's instructions (Thermo Fisher Scientific). Direct labeling of antibodies with Alexa Fluor fluorophores was performed using an antibody-labeling kit according to the manufacturer's instructions (Invitrogen). Vybrant C_{18}DiD was also from Invitrogen.

Bovine plasma FN and laminin were purchased from Sigma-Aldrich, and the recombinant 50K fragment of FN comprising type III repeats 6–10 was made as described previously (Mould et al., 1997). The Cys-Arg-Arg-Glu-Thr-Ala-Trp-Ala-Cys (CRRETAWAC) peptide was purchased from Peptide 2.0 Inc. and was cyclized before conjugating to rabbit IgG using BS^3 (bis[sulfosuccinimidyl] suberate; Thermo Fisher Scientific) as described previously (Humphries et al., 2000). The production of recombinant soluble α5β1-Fc has been described previously (Coe et al., 2001). The α5-Fc and β1-Fc used in these experiments comprised residues 1–951 of α5, and residues 1–708 of β1 and each subunit was fused to a human Fc domain mutated to facilitate heterodimerization of the subunits. To allow removal of the Fc domain, a Tobacco Etch Virus (TEV) cleavage site was included between the integrin sequence and the Fc domain in the β1 construct only. If required, the integrin was purified on protein A–Sepharose (GE Healthcare) and the Fc domain removed from the β subunit with TEV protease (Invitrogen) according to the manufacturer's instructions.

Full-length α5CFP cDNA was provided by A.R. Horwitz (University of Virginia, Charlottesville, VA). β1YFP was obtained by cloning the β1 cDNA from β1-GFP (Parsons et al., 2008) into a pCDNA3 vector containing eYFP. Mutation of both soluble and full-length α5β1 was performed by site-directed mutagenesis using QuikChange XL kit (Agilent Technologies) according to the manufacturer's instructions.

HFFs (provided by K. Clark, University of Leicester, UK) and GD25 cells (provided by R. Fässler, Max Planck Institute for Biochemistry, Martinsried, Germany) were maintained in Dulbecco's minimal essential medium (Sigma-Aldrich) supplemented with 10% fetal calf serum and 2 mM L-glutamine. GD25 cells were transfected with plasmid DNA using Lipofectamine 2000 reagent (Invitrogen) according to the manufacturer's instructions.

Fc-capture ELISA to compare epitope expression and ligand binding by α5β1-Fc heterodimers

Binding of antibodies and 50K ligand to soluble α5β1-Fc proteins was performed by Fc-capture ELISA as described previously (Mould et al., 2003a). In brief, 96-well plates (Costar) were coated with goat anti–human γ1 Fc (Jackson Immunochemicals) then blocked with 5% (wt/vol) BSA in Tris-buffered saline (TBS). Tissue culture supernatant from integrin-transfected

cells was added and incubated at room temperature for 1 h. The plate was then washed with TBS and 10 µg/ml of primary antibody added. After a further 45 min incubation, the plate was washed again and the bound antibody quantitated by addition of 1:1,000 anti–mouse or anti–rat IgG peroxidase conjugate (Jackson Immunochemicals) followed by 2,2′-azinobis(3-ethylbenzothiazoline-6-sulfonic acid) substrate (ABTS; Sigma-Aldrich). Absorbance was read at 405 nm. For experiments measuring ligand binding to WT and mutant α5β1-Fc constructs, 50K fragment of FN was biotinylated using sulfo-long chain-*N*-hydroxysuccinimido biotin (Thermo Fisher Scientific) as described previously (Mould et al., 1997) and used at 0.5 µg/ml, either with or without the addition of activating anti-α5 or β1 antibodies at 10 µg/ml. Binding of ligand was quantitated by adding 1:500 extravidin-peroxidase conjugate (Sigma-ALdrich) followed by ABTS as above. Background binding to wells incubated with supernatant from mock-transfected cells was subtracted from all measurements. In assays involving a comparison between different α5β1-Fc integrin constructs, binding levels of the neutral anti-β1 antibody K20 were used to normalize for any differences between the amounts of integrin heterodimers bound to the wells as described previously (Mould et al., 2003a).

Immunofluorescence

Cells were plated onto glass-bottom dishes (MatTek) precoated with ligand and allowed to spread for 60 min in serum-free culture medium. Transiently transfected GD25 cells were used 24–36 h after transfection. Cells were fixed with 3% (wt/vol) paraformaldehyde for 15 min, permeabilized for 5 min with 0.5% (wt/vol) Triton X-100 (Sigma-Aldrich), and subsequently incubated for 45 min with the appropriate Alexa Fluor antibody conjugate. After washing in PBS, cells were imaged at room temperature using a DeltaVision system (Applied Precision) comprising a widefield inverted microscope (model IX-70; Olympus) with a 100x/1.35 UPLAN APO objective. Images were captured using a CCD camera (model CH350; Photometrics) and Softworx analysis software (Applied Precision). Subsequent image analysis and processing were performed using ImageJ and Adobe Photoshop software. For assays using CRRETAWAC-IgG as ligand, the plates were coated with 100 µg/ml of the peptide ligand and blocked with 10 mg/ml heat-denatured bovine serum albumin (Sigma-Aldrich) before addition of cells.

FLIM-based FRET analysis

HFFs were allowed to spread on FN-coated glass-bottom dishes (MatTek) for 1 h in serum-free medium and then for a further 15 min in the presence of Vybrant C_{18}DiD at a final concentration of 5 µM to label the cell membrane. The cells were washed and fixed with 3% (wt/vol) PFA and stained with a Fab fragment of VC5 directly conjugated to Alexa Fluor 546 as described above. C_{18}DiD and Alexa 546 have single photon absorption and fluorescence emission spectra sufficiently separated so that their fluorescence can be excited and detected separately while an overlap between the emission spectrum of Alexa 546 and the absorption spectrum of C_{18}DiD allows these two dyes to act as a FRET pair.

Fluorescence lifetime images of Alexa Fluor 546–labeled cells, either with or without acceptor (DiD), were acquired at room temperature using a purpose-built laser scanning confocal microscope equipped with time-correlated single photon counting (TCSPC) electronics (SPC-730, Becker-Hickl GmbH). The microscope incorporated an inverted microscope body (Axiovert 135; Carl Zeiss, Inc.) with a 40x/1.3NA FLUAR objective (Carl Zeiss, Inc.), and was used to acquire both FLIM and intensity images. Alexa 546 was excited with 545-nm pulsed laser light (Coherent, MIRA-OPO, 76-Mhz repetition rate) and the Alexa 546 fluorescence was detected at 560–610 nm using a fast photomultiplier tube (PMC-100; Becker-Hickl GmbH). The resulting time-resolved images were analyzed using SPCImage (Becker-Hickl GmbH) FLIM analysis software. Fluorescent intensity decays were fitted to a single exponential decay model where acceptor was absent and a bi-exponential model when both donor and acceptor were present, to extract mean lifetimes. The reduced χ^2 parameter was used to judge the goodness of fit, which was deemed acceptable for $0.8 < \chi^2 < 1.2$. For each area of interest, lifetime measurements for donor only or donor in the presence of acceptor were obtained by taking the mean of the distribution of lifetimes of cell membrane pixels. For bi-exponential fits, these lifetimes were the weighted mean of the two fitted lifetime components.

In the case of FLIM acquisitions of cells labeled with both donor and acceptor, a corresponding confocal image of C_{18}DiD was taken afterward. A 639-nm CW laser (PTI) was used to directly excite the membrane-localized DiD and the emitted fluorescence collected at >670 nm from the same field of view as the FLIM data, using an R3896 photomultiplier tube (Hamamatsu Photonics). Acceptor intensity was normalized to the 639-nm laser power at the time of measurement.

FRET efficiencies were calculated from the measured donor lifetimes using the equation $E_{FRET} = 1 - (\tau_{DA}/\tau_D)$, where τ_{DA} and τ_D are the mean donor lifetimes in the presence and absence of acceptor, respectively. The Förster radius, R_0 (the separation of a single donor and acceptor at which the FRET efficiency is 0.5) for Alexa 546 and C_{18}DiD was calculated to be 6.6 nm using spectral data obtained from Invitrogen and the value of the orientation factor corresponding to the dynamic averaging limit. The steady-state anisotropy of C_{18}DiD molecules in lipid vesicles was measured using an L-format Jobin-Yvon Fluorolog fluorimeter with a Xenon lamp as a light source and found to be 0.154 compared with the maximum possible value for static dye molecules of 0.4 (Lakowicz, 1983), indicating free rotation of the DiD dye molecules. For FRET pairs where both fluorophores exhibit anisotropies <0.22, the error introduced by using the dynamic averaging value to calculate the Förster radius is <10% (Haas et al., 1978). The dye/protein (f:p) molar ratio of the labeled Fabs was calculated to be almost equal at 1.18 fluorophore:1 of Fab fragment.

To determine acceptor densities from the measured fluorescence intensity of C_{18}DiD, FLIM-FRET measurements were performed on samples of C_{18}DiI (donor) and C_{18}DiD (acceptor) randomly distributed in a monolayer of phosphatidylcholine. The acceptor was purposely photobleached to obtain a plot of E_{FRET} versus acceptor fluorescence intensity. These data were fitted to the FRET efficiency as a function of acceptor density for a zero distance of closest approach of donors and acceptors calculated by Wolber and Hudson (1979), $E_{FRET} = 1 - (0.6463e^{-4.7497D} + 0.3537e^{-20168D})$ and $D = KI$, where K is a constant factor relating the fluorescence intensity, I and acceptor density, D (in units of acceptors per R_0^2). The value of K found was then used to calculate acceptor densities from the measured C_{18}DiD intensities, an approach that has been used previously (Carraway et al., 1990; Chigaev et al., 2003).

Statistical analysis

The Student's *t* test was used to test statistical significance between two groups of data and values <0.05 were taken as significant.

Online supplemental material

Fig. S1 A shows the ratio of VC5–Alexa 546 fluorescence to α5CFP fluorescence in WT and LT α5β1 at different locations. Fig. S1 B shows the fluorescence intensity of DiD staining in focal adhesions and the cell membrane. Fig. S2 shows the effect of both photobleaching and increasing proportions of unlabeled VC5 on the lifetime of VC5–Alexa 546 in adhesion complexes and the cell membrane. Fig. S3 shows flow cytometry analysis of the conformation of LT α5β1 assessed by 9EG7 binding. Fig. S4 A shows the localization of mouse α5 to adhesion complexes in GD25 cells expressing WT or LT α5β1. Fig. S4 B shows the spreading of HFF cells on CRRETAWAC-IgG. Online supplemental material is available at http://www.jcb.org/cgi/content/full/jcb.200907174/DC1.

We would like to thank Ralph Isberg for VC5 antibody and Sue Craig for preparing Fab fragments. Thanks also to Pat Buckley for preparing the homology model of α5β1 and to Paul Mould for helpful discussions.

This work was supported by grants 045225 and 074941 from the Wellcome Trust (to M.J. Humphries). The Bioimaging Facility microscopes used in this study were purchased with grants from the Biotechnology and Biological Sciences Research Council, Wellcome, and the University of Manchester Strategic Fund.

Submitted: 31 July 2009
Accepted: 23 February 2010

References

Adair, B.D., J.P. Xiong, C. Maddock, S.L. Goodman, M.A. Arnaout, and M. Yeager. 2005. Three-dimensional EM structure of the ectodomain of integrin αVβ3 in a complex with fibronectin. *J. Cell Biol.* 168:1109–1118. doi:10.1083/jcb.200410068

Amiot, M., A. Bernard, H.C. Tran, G. Leca, J.M. Kanellopoulos, and L. Boumsell. 1986. The human cell surface glycoprotein complex (gp 120,200) recognized by monoclonal antibody K20 is a component binding to phytohaemagglutinin on T cells. *Scand. J. Immunol.* 23:109–118. doi:10.1111/j.1365-3083.1986.tb01948.x

Bazzoni, G., D.T. Shih, C.A. Buck, and M.E. Hemler. 1995. Monoclonal antibody 9EG7 defines a novel β 1 integrin epitope induced by soluble ligand and manganese, but inhibited by calcium. *J. Biol. Chem.* 270:25570–25577. doi:10.1074/jbc.270.30.17784

Bazzoni, G., L. Ma, M.L. Blue, and M.E. Hemler. 1998. Divalent cations and ligands induce conformational changes that are highly divergent among beta1 integrins. *J. Biol. Chem.* 273:6670–6678. doi:10.1074/jbc.273.12.6670

Beglova, N., S.C. Blacklow, J. Takagi, and T.A. Springer. 2002. Cysteine-rich module structure reveals a fulcrum for integrin rearrangement upon activation. *Nat. Struct. Biol.* 9:282–287. doi:10.1038/nsb779

Bunch, T.A. 2010. Integrin αIIbß3 activation in CHO cells and platelets increases clustering rather than affinity. *J. Biol. Chem.* 285:1841–1849. doi:10.1074/jbc.M109.057349

Calzada, M.J., M.V. Alvarez, and J. Gonzalez-Rodriguez. 2002. Agonist-specific structural rearrangements of integrin α IIbbeta 3. Confirmation of the bent conformation in platelets at rest and after activation. *J. Biol. Chem.* 277:39899–39908. doi:10.1074/jbc.M205886200

Carraway, K.L. III, J.G. Koland, and R.A. Cerione. 1990. Location of the epidermal growth factor binding site on the EGF receptor. A resonance energy transfer study. *Biochemistry.* 29:8741–8747. doi:10.1021/bi00489a034

Chigaev, A., T. Buranda, D.C. Dwyer, E.R. Prossnitz, and L.A. Sklar. 2003. FRET detection of cellular α4-integrin conformational activation. *Biophys. J.* 85:3951–3962. doi:10.1016/S0006-3495(03)74809-7

Chigaev, A., A. Waller, G.J. Zwartz, T. Buranda, and L.A. Sklar. 2007. Regulation of cell adhesion by affinity and conformational unbending of α4β1 integrin. *J. Immunol.* 178:6828–6839.

Clark, K., R. Pankov, M.A. Travis, J.A. Askari, A.P. Mould, S.E. Craig, P. Newham, K.M. Yamada, and M.J. Humphries. 2005. A specific α5β1-integrin conformation promotes directional integrin translocation and fibronectin matrix formation. *J. Cell Sci.* 118:291–300. doi:10.1242/jcs.01623

Cluzel, C., F. Saltel, J. Lussi, F. Paulhe, B.A. Imhof, and B. Wehrle-Haller. 2005. The mechanisms and dynamics of (α)v(β)3 integrin clustering in living cells. *J. Cell Biol.* 171:383–392. doi:10.1083/jcb.200503017

Coe, A.P., J.A. Askari, A.D. Kline, M.K. Robinson, H. Kirby, P.E. Stephens, and M.J. Humphries. 2001. Generation of a minimal α5β1 integrin-Fc fragment. *J. Biol. Chem.* 276:35854–35866. doi:10.1074/jbc.M103639200

Coutinho, A., C. García, J. González-Rodríguez, and M.P. Lillo. 2007. Conformational changes in human integrin alphaIIbbeta3 after platelet activation, monitored by FRET. *Biophys. Chem.* 130:76–87. doi:10.1016/j.bpc.2007.07.007

Friedland, J.C., M.H. Lee, and D. Boettiger. 2009. Mechanically activated integrin switch controls alpha5beta1 function. *Science.* 323:642–644. doi:10.1126/science.1168441

Haas, E., E. Katchalski-Katzir, and I.Z. Steinberg. 1978. Effect of the orientation of donor and acceptor on the probability of energy transfer involving electronic transitions of mixed polarization. *Biochemistry.* 17:5064–5070. doi:10.1021/bi00616a032

Hughes, P.E., F. Diaz-Gonzalez, L. Leong, C. Wu, J.A. McDonald, S.J. Shattil, and M.H. Ginsberg. 1996. Breaking the integrin hinge. A defined structural constraint regulates integrin signaling. *J. Biol. Chem.* 271:6571–6574. doi:10.1074/jbc.271.12.6571

Humphries, M.J. 2004. Monoclonal antibodies as probes of integrin priming and activation. *Biochem. Soc. Trans.* 32:407–411. doi:10.1042/BST0320407

Humphries, J.D., J.A. Askari, X.-P. Zhang, Y. Takada, M.J. Humphries, and A.P. Mould. 2000. Molecular basis of ligand recognition by integrin α5β 1. II. Specificity of arg-gly-Asp binding is determined by Trp157 of the α subunit. *J. Biol. Chem.* 275:20337–20345. doi:10.1074/jbc.M000568200

Hynes, R.O. 2002. Integrins: bidirectional, allosteric signaling machines. *Cell.* 110:673–687. doi:10.1016/S0092-8674(02)00971-6

Iwasaki, K., K. Mitsuoka, Y. Fujiyoshi, Y. Fujisawa, M. Kikuchi, K. Sekiguchi, and T. Yamada. 2005. Electron tomography reveals diverse conformations of integrin alphaIIbbeta3 in the active state. *J. Struct. Biol.* 150:259–267. doi:10.1016/j.jsb.2005.03.005

Kamata, T., M. Handa, Y. Sato, Y. Ikeda, and S. Aiso. 2005. Membrane-proximal alpha/beta stalk interactions differentially regulate integrin activation. *J. Biol. Chem.* 280:24775–24783. doi:10.1074/jbc.M409548200

Kim, M., C.V. Carman, and T.A. Springer. 2003. Bidirectional transmembrane signaling by cytoplasmic domain separation in integrins. *Science.* 301:1720–1725. doi:10.1126/science.1084174

Kim, M., C.V. Carman, W. Yang, A. Salas, and T.A. Springer. 2004. The primacy of affinity over clustering in regulation of adhesiveness of the integrin αLβ2. *J. Cell Biol.* 167:1241–1253. doi:10.1083/jcb.200404160

Kong, F., A.J. García, A.P. Mould, M.J. Humphries, and C. Zhu. 2009. Demonstration of catch bonds between an integrin and its ligand. *J. Cell Biol.* 185:1275–1284. doi:10.1083/jcb.200810002

Lakowicz, J.R. 1983. Principles of Fluorescence Spectroscopy. 2nd Ed. Kluwer Academic / Plenum Publishers. 725 pp.

LaFlamme, S.E., S.K. Akiyama, and K.M. Yamada. 1992. Regulation of fibronectin receptor distribution. *J. Cell Biol.* 117:437–447. doi:10.1083/jcb.117.2.437

Lefort, C.T., Y.M. Hyun, J.B. Schultz, F.-Y. Law, R.E. Waugh, P.A. Knauf, and M. Kim. 2009. Outside-in signal transmission by conformational changes in integrin Mac-1. *J. Immunol.* 183:6460–6468. doi:10.4049/jimmunol.0900983

Lenter, M., H. Uhlig, A. Hamann, P. Jenö, B. Imhof, and D. Vestweber. 1993. A monoclonal antibody against an activation epitope on mouse integrin chain β 1 blocks adhesion of lymphocytes to the endothelial integrin α 6 β 1. *Proc. Natl. Acad. Sci. USA.* 90:9051–9055. doi:10.1073/pnas.90.19.9051

Lu, C., M. Ferzly, J. Takagi, and T.A. Springer. 2001. Epitope mapping of antibodies to the C-terminal region of the integrin β 2 subunit reveals regions that become exposed upon receptor activation. *J. Immunol.* 166:5629–5637.

Luo, B.-H., T.A. Springer, and J. Takagi. 2004. A specific interface between integrin transmembrane helices and affinity for ligand. *PLoS Biol.* 2:e153. doi:10.1371/journal.pbio.0020153

Martin-Fernandez, M., D.T. Clarke, M.J. Tobin, S.V. Jones, and G.R. Jones. 2002. Preformed oligomeric epidermal growth factor receptors undergo an ectodomain structure change during signaling. *Biophys. J.* 82:2415–2427. doi:10.1016/S0006-3495(02)75585-9

Mould, A.P., S.K. Akiyama, and M.J. Humphries. 1995. Regulation of integrin α 5 β 1-fibronectin interactions by divalent cations. Evidence for distinct classes of binding sites for Mn^{2+}, Mg^{2+}, and Ca^{2+}. *J. Biol. Chem.* 270:26270–26277. doi:10.1074/jbc.270.44.26270

Mould, A.P., J.A. Askari, S. Aota, K.M. Yamada, A. Irie, Y. Takada, H.J. Mardon, and M.J. Humphries. 1997. Defining the topology of integrin α5β1-fibronectin interactions using inhibitory anti-α5 and anti-β1 monoclonal antibodies. Evidence that the synergy sequence of fibronectin is recognized by the amino-terminal repeats of the α5 subunit. *J. Biol. Chem.* 272:17283–17292. doi:10.1074/jbc.272.28.17283

Mould, A.P., J.A. Askari, S.J. Barton, A.D. Kline, P.A. McEwan, S.E. Craig, and M.J. Humphries. 2002. Integrin activation involves a conformational change in the α 1 helix of the β subunit A-domain. *J. Biol. Chem.* 277:19800–19805. doi:10.1074/jbc.M201571200

Mould, A.P., S.J. Barton, J.A. Askari, P.A. McEwan, P.A. Buckley, S.E. Craig, and M.J. Humphries. 2003a. Conformational changes in the integrin β A domain provide a mechanism for signal transduction via hybrid domain movement. *J. Biol. Chem.* 278:17028–17035. doi:10.1074/jbc.M213139200

Mould, A.P., E.J. Symonds, P.A. Buckley, J.G. Grossmann, P.A. McEwan, S.J. Barton, J.A. Askari, S.E. Craig, J. Bella, and M.J. Humphries. 2003b. Structure of an integrin-ligand complex deduced from solution x-ray scattering and site-directed mutagenesis. *J. Biol. Chem.* 278:39993–39999. doi:10.1074/jbc.M304627200

Mould, A.P., M.A. Travis, S.J. Barton, J.A. Hamilton, J.A. Askari, S.E. Craig, P.R. Macdonald, R.A. Kammerer, P.A. Buckley, and M.J. Humphries. 2005. Evidence that monoclonal antibodies directed against the integrin β subunit plexin/semaphorin/integrin domain stimulate function by inducing receptor extension. *J. Biol. Chem.* 280:4238–4246. doi:10.1074/jbc.M412240200

Nishida, N., C. Xie, M. Shimaoka, Y. Cheng, T. Walz, and T.A. Springer. 2006. Activation of leukocyte β2 integrins by conversion from bent to extended conformations. *Immunity.* 25:583–594. doi:10.1016/j.immuni.2006.07.016

Parsons, M., A.J. Messent, J.D. Humphries, N.O. Deakin, and M.J. Humphries. 2008. Quantification of integrin receptor agonism by fluorescence lifetime imaging. *J. Cell Sci.* 121:265–271. doi:10.1242/jcs.018440

Partridge, A.W., S. Liu, S. Kim, J.U. Bowie, and M.H. Ginsberg. 2005. Transmembrane domain helix packing stabilizes integrin alphaIIbbeta3 in the low affinity state. *J. Biol. Chem.* 280:7294–7300. doi:10.1074/jbc.M412701200

Puklin-Faucher, E., M. Gao, K. Schulten, and V. Vogel. 2006. How the headpiece hinge angle is opened: New insights into the dynamics of integrin activation. *J. Cell Biol.* 175:349–360. doi:10.1083/jcb.200602071

Ridgway, J.B., L.G. Presta, and P. Carter. 1996. 'Knobs-into-holes' engineering of antibody CH3 domains for heavy chain heterodimerization. *Protein Eng.* 9:617–621. doi:10.1093/protein/9.7.617

Rocco, M., C. Rosano, J.W. Weisel, D.A. Horita, and R.R. Hantgan. 2008. Integrin conformational regulation: uncoupling extension/tail separation from changes in the head region by a multiresolution approach. *Structure.* 16:954–964. doi:10.1016/j.str.2008.02.019

Shattil, S.J., H. Kashiwagi, and N. Pampori. 1998. Integrin signaling: the platelet paradigm. *Blood.* 91:2645–2657.

Shi, M., S.Y. Foo, S.M. Tan, E.P. Mitchell, S.K. Law, and J. Lescar. 2007. A structural hypothesis for the transition between bent and extended conformations of the leukocyte β2 integrins. *J. Biol. Chem.* 282:30198–30206. doi:10.1074/jbc.M701670200

Stryer, L., and R.P. Haugland. 1967. Energy transfer: a spectroscopic ruler. *Proc. Natl. Acad. Sci. USA.* 58:719–726. doi:10.1073/pnas.58.2.719

Takagi, J., H.P. Erickson, and T.A. Springer. 2001. C-terminal opening mimics 'inside-out' activation of integrin alpha5beta1. *Nat. Struct. Biol.* 8:412–416. doi:10.1038/87569

Takagi, J., B.M. Petre, T. Walz, and T.A. Springer. 2002. Global conformational rearrangements in integrin extracellular domains in outside-in and inside-out signaling. *Cell.* 110:599–11. doi:10.1016/S0092-8674(02)00935-2

Takagi, J., K. Strokovich, T.A. Springer, and T. Walz. 2003. Structure of integrin α5β1 in complex with fibronectin. *EMBO J.* 22:4607–4615. doi:10.1093/emboj/cdg445

Tran Van Nhieu, G., and R.R. Isberg. 1993. Bacterial internalization mediated by β 1 chain integrins is determined by ligand affinity and receptor density. *EMBO J.* 12:1887–1895.

Wegener, K.L., A.W. Partridge, J. Han, A.R. Pickford, R.C. Liddington, M.H. Ginsberg, and I.D. Campbell. 2007. Structural basis of integrin activation by talin. *Cell.* 128:171–182. doi:10.1016/j.cell.2006.10.048

Wennerberg, K., L. Lohikangas, D. Gullberg, M. Pfaff, S. Johansson, and R. Fässler. 1996. β 1 integrin-dependent and -independent polymerization of fibronectin. *J. Cell Biol.* 132:227–238. doi:10.1083/jcb.132.1.227

Wolber, P.K., and B.S. Hudson. 1979. An analytic solution to the Förster energy transfer problem in two dimensions. *Biophys. J.* 28:197–210. doi:10.1016/S0006-3495(79)85171-1

Xiao, T., J. Takagi, B.S. Coller, J.H. Wang, and T.A. Springer. 2004. Structural basis for allostery in integrins and binding to fibrinogen-mimetic therapeutics. *Nature.* 432:59–67. doi:10.1038/nature02976

Xiong, J.-P., T. Stehle, B. Diefenbach, R. Zhang, R. Dunker, D.L. Scott, A. Joachimiak, S.L. Goodman, and M.A. Arnaout. 2001. Crystal structure of the extracellular segment of integrin α Vbeta3. *Science.* 294:339–345. doi:10.1126/science.1064535

Ye, F., G. Hu, D. Taylor, B. Ratnikov, A.A. Bobkov, M.A. McLean, S.G. Sligar, K.A. Taylor, and M.H. Ginsberg. 2010. Recreation of the terminal events in physiological integrin activation. *J. Cell Biol.* 188:157–173. doi:10.1083/jcb.200908045

Zhu, J., C.V. Carman, M. Kim, M. Shimaoka, T.A. Springer, and B.H. Luo. 2007. Requirement of α and β subunit transmembrane helix separation for integrin outside-in signaling. *Blood.* 110:2475–2483. doi:10.1182/blood-2007-03-080077

Zhu, J., B.H. Luo, T. Xiao, C. Zhang, N. Nishida, and T.A. Springer. 2008. Structure of a complete integrin ectodomain in a physiologic resting state and activation and deactivation by applied forces. *Mol. Cell.* 32:849–861. doi:10.1016/j.molcel.2008.11.018